Published in final edited form as:
J Alzheimers Dis. 2014 ; 39(1): 145–162. doi:10.3233/JAD-131238.

Experimental Induction of Type 2 Diabetes in Aging-Accelerated Mice Triggered Alzheimer-Like Pathology and Memory Deficits

Jogender Mehla[a,b], **Balwantsinh C. Chauhan**[c], and **Neelima B. Chauhan**[a,b,*]

[a]Neuroscience Research, Jesse Brown VA Medical Center, Chicago, IL, USA

[b]Department of Pediatrics, University of Illinois Hospital & Health Science System-Children's Hospital, University of Illinois at Chicago, Chicago, IL, USA

[c]Department of Biopharmaceutical Sciences, Roosevelt University, Schaumburg, IL, USA

Abstract

Alzheimer's disease (AD) is an age-dependent neurodegenerative disease constituting ~95% of late-onset non-familial/sporadic AD, and only ~5% accounting for early-onset familial AD. Availability of a pertinent model representing sporadic AD is essential for testing candidate therapies. Emerging evidence indicates a causal link between diabetes and AD. People with diabetes are >1.5-fold more likely to develop AD. Senescence-accelerated mouse model (SAMP8) of accelerated aging displays many features occurring early in AD. Given the role played by diabetes in the pre-disposition of AD, and the utility of SAMP8 non-transgenic mouse model of accelerated aging, we examined if high fat diet-induced experimental type 2 diabetes in SAMP8 mice will trigger pathological aging of the brain. Results showed that compared to non-diabetic SAMP8 mice, diabetic SAMP8 mice exhibited increased cerebral amyloid-β, dysregulated tau-phosphorylating glycogen synthase kinase 3β, reduced synaptophysin immunoreactivity, and displayed memory deficits, indicating Alzheimer-like changes. High fat diet-induced type 2 diabetic SAMP8 mice may represent the metabolic model of AD.

Keywords

Alzheimer's disease; amyloid-β; diabetes; glycogen synthase kinase-3β; learning and memory; pathological aging of the brain; senescence-accelerated mice; synaptophysin; tau

INTRODUCTION

Alzheimer's disease (AD) is an age-dependent heterogeneous neurodegenerative disorder functionally characterized by mild cognitive impairment at its onset with progressive cognitive decline; and pathologically characterized by progressive deposition of amyloid-β (Aβ) neuritic plaques derived from amyloid-β protein precursor (AβPP), and neurofibrillary tangles derived from abnormal phosphorylation of tau proteins, within the brain parenchyma [1, 2]. Aβ is formed after sequential cleavage of AβPP by the proteolytic enzymes β- and γ-secretases. The γ-secretase cleavage at the C-terminal end of the transmembrane region of AβPP generates a number of isoforms of 36–43 amino acid residues. The most abundant isoforms are $Aβ_{40}$ and $Aβ_{42}$. Initially produced Aβ forms are non-fibrillar/soluble (soluble

*Correspondence to: Neelima B. Chauhan, Ph.D., Neuroscience Research (151), Jesse Brown VA Medical Center, 820 South Damen Avenue, Chicago, IL 60612, USA. Tel.: +1 312 569 7747; Fax: +1 312 569 8114; nchauhan@uic.edu.

Authors' disclosures available online (http://www.j-alz.com/disclosures/view.php?id=1935).

$A\beta_{40}$ and soluble $A\beta_{42}$), which eventually undergo fibrillation to produce fibrillar forms of Aβ [1, 2].

According to the Alzheimer's Association Facts and Figures, AD is the sixth leading cause of death in the United States with ~5.4 million Americans (and ~36 million people worldwide) suffering from AD, with someone developing AD every 69 s and an annual economic burden of ~$200 billion. By the middle of the century, these numbers are estimated to triple with the projection of >15 million Americans (and >115 million people worldwide) afflicted with AD at a rate of every 33 s someone developing AD along with the increased economic burden of ~$1.1 trillion per year, if effective treatments are not discovered. Out of 5.4 million Americans with AD, ~5.2 million are suffering from late onset sporadic AD, while the remaining ~200,000 AD patients are diagnosed with early onset familial AD, indicating that the vast majority (~95%) of diagnosed AD cases are sporadic in origin while the rest (~5%) are of familial origin, emphasizing the role played by non-genetic environmental or metabolic factors in triggering pathological aging of the brain leading to late onset AD [3–6].

Emerging epidemiological data indicate that type 2 diabetes (T2DM) is a significant comorbid risk factor for developing late onset AD [4, 5, 7], suggesting a causal link between insulin dysfunction and AD pathogenesis [5, 8–11]. A growing body of evidence suggests that insulin dyshomeostasis is fundamental to the development of sporadic AD [4, 12–19], designating sporadic AD as type 3 diabetes [20–22]. T2DM and AD share several commonalities including impaired glucose metabolism, increased oxidative stress, inflammation, insulin resistance, and amyloidosis, contributing to the overlapping pathology and thereby compounding disease symptoms and progression [23]. The risk of developing AD in diabetic patients remains strong even when vascular factors are regulated, suggesting a non-vascular role of insulin in inducing AD pathogenesis [24]. Several non-vascular factors seem to contribute to the increased risk of AD in T2DM, including defects in insulin signaling, increased production and reduced degradation of Aβ, and hyperphosphorylation of tau protein [24, 25].

Earlier studies have demonstrated that altered cerebral glucose metabolism [4, 26] and insulin resistance/hyperinsulinemia [9, 12, 13, 15, 16, 27] restrict Aβ degrading ability of insulin degrading enzyme [28] and glucagon-like peptide-1 [29]. In addition, insulin resistance has been shown to upregulate AβPP resulting in the overproduction of Aβ multimers [30] and impaired clearance of Aβ [31], eventually exerting synaptotoxicity [32–34]. People with diabetes are >1.5-fold more likely to develop AD than individuals without diabetes [16, 35, 36]. However, insulin dysfunction by itself is not sufficient to cause AD pathogenesis, as indicated by the study in which high fat diet-induced T2DM in young C57BL/6J mice did not produce AD-like pathology [37], emphasizing that insulin dysfunction may not be adequate by itself to cause AD-like changes, unless accompanied with aging, a major risk factor for AD [38]. Thus, T2DM seems to constitute one of the major risk factors that may tip the balance from normal aging of brain to the pathological aging of the brain.

Effective disease-modifying therapies are needed to prevent the projected epidemic of AD worldwide. In order to validate effective therapies, availability of a pertinent model system is critical. Current modeling of AD is restricted to the expression of AD-related pathology associated with specific mutations observed in early-onset familial AD [39, 40], which represents only ~5% of diagnosed AD cases. To date there are no models representing late-onset age-related non-familial/sporadic AD, the feature that accounts for the vast majority (~95%) of AD cases. Senescence-accelerated mouse model (SAMP8) of accelerated aging displays many features known to occur early in the pathogenesis of AD and hence are

considered an excellent model for studying aging neurodegenerative changes associated with AD [41–43]. Given the possible role played by T2DM in the pre-disposition of AD, and the utility of SAMP8 mouse model of accelerated aging, we investigated if experimental induction of T2DM in SAMP8 (diabetic SAMP8 mice) will accentuate their already existing neurodegenerative features, and trigger pathological aging of the brain, reflecting characteristic neuropathological and cognitive impairments observed in AD.

MATERIALS AND METHODS

Animals and treatment

3-month-old SAMP8 (n = 10) (accelerated aging) and SAMPR1 (n = 10) (aging resistant) mice were obtained from Harlan (Indianapolis, IN) and used in this study. Earlier reports indicated that the AKR background strain in particular (background strain of SAMP8 and SAMPR1 mice) is the insulin resistant strain, which develops diabetes after 8 weeks of high fat diet feeding [44]; unlike other strains, such as BDF1 or C57, which develop diabetes after 14+ weeks of high fat diet feeding [45–48]. Consistent with these reports, we confirmed that feeding of SAMP8 (n = 5) and SAMPR1 (n = 5) mice with high fat diet (HF; fat 60 Kcal%, carbohydrates 20 Kcal%, proteins 20 Kcal%, Research Diets, NJ) for 8 weeks resulted in the development of experimental T2DM. Controls [SAMP8 (n = 5) and SAMPR1 (n = 5)] were fed with low fat control diet (LF; fat 10 Kcal%, carbohydrates 70 Kcal%, proteins 20 Kcal%, Research Diets, NJ) for the same duration. The animals were continued to be fed with HF diet for 4 additional weeks to investigate the effect of sustained experimental T2DM on aging of the brain. Development of diabetes was monitored by weekly measurements of fasting blood glucose (Abbott Precision), serum insulin levels, and blood levels of glycosylated hemoglobin (HbA1c) (Crystal Chem, Inc.) (Table 1). In addition, a glucose tolerance test (Abbott Precision) was performed at 8 weeks (Diabetic stage) and 12 weeks (Sustained diabetes-Treatment end point stage) of HF treatment (Fig. 1).

At the end of 12 weeks HF treatment, mice were evaluated for learning (Fig. 2), memory (Fig. 3), and spontaneous exploration (Fig. 4), and then euthanized. Brains were divided in two longitudinal halves. One hemibrain was analyzed by enzyme-linked immonosorbent assay (ELISA) for measuring soluble $A\beta_{40}$ ($sA\beta_{40}$) and $sA\beta_{42}$ (Fig. 5); and for western blot analysis of the most prominent tau-phosphorylating kinase glycogen synthase kinase 3β (GSK3β) (Fig. 8). The remaining hemibrain was analyzed for immunohistochemistry of Aβ, phospho-tau (Figs. 6 and 7), and synaptophysin (Figs. 9 and 10).

An additional set of animals consisted of SAMP8 (n = 5) and SAMPR1 (n = 5) mice fed with HF (fat 60 Kcal%, carbohydrates 20 Kcal%, proteins 20 Kcal%, Research Diets, NJ) for 12 weeks; and controls [SAMP8 (n = 5) and SAMPR1 (n = 5)] fed with LF (fat 10 Kcal %, carbohydrates 70 Kcal%, proteins 20 Kcal%, Research Diets, NJ) for the same duration. Blood HbA1c levels were measured each week for 12 weeks up to the treatment-end point (Table 1). At the end of 12 weeks of dietary treatment, mice were euthanized. Each hemibrain was processed separately to measure cerebral levels of insulin (Crystal Chem, Inc.) and to measure cytochrome c oxidase and pyruvate dehydrogenase (Abcam.com) as per manufacturer's instructions, and analyzed using commercial kits (Table 1).

All animal procedures were performed in accordance with the National Research Council's guidelines, and in accordance with the institutional animal care and use committee(s) from the University of Illinois at Chicago and Jesse Brown VA Medical Center Chicago.

Spatial acquisition learning, and memory assessment

Morris water maze testing for spatial acquisition of place and cue learning, a task thought to involve hippocampus, was performed as established [49–52]. Morris water maze is a circular pool of water of 1.4 m diameter filled with water maintained at 25° C. The floor of the pool was divided into imaginary 3 annuli and 4 quadrants. An indiscernible platform made up of transparent acrylic was placed in one of the quadrants, 1 cm below the surface of water. Prior to spatial learning, mice were handled to get acclimatized to the experimenter and surroundings. Then the mice were subjected to experimental trials (6 trials per day for 3 days). During daily training, each animal was admitted in the pool facing the pool wall with a randomly selected start point on the opposite side of the platform quadrant and allowed to swim for a maximum of 60 s to locate the submerged platform. The time required for locating the submerged platform was termed “Latency”. Latency for each animal per day was recorded and averaged across number of trials/day. A group mean was derived from individual averages.

Shorter latencies indicated that the spatial learning involving hippocampus was not deteriorated (acquisition), while longer latencies indicated spatial learning disability. On the fifth day following the last acquisition trial, retention of the spatial memory was tested. Each animal was given only one probe trial of 60 s duration. The submerged platform was removed from its usual location, and the animal was expected to enter the target quadrant and make more entries into this location which previously contained the platform, indicating whether or not the original location of the submerged platform was still retained by the trained animal (memory retention). Time spent searching for the platform in the target quadrant which previously contained the platform, length of swim path and swim speed, and the time spent in non-target quadrants were recorded by video tracking. Individual values were used to derive group means and analyzed.

Spontaneous exploration working memory assessment

The Y-maze test for evaluating spontaneous alteration behavior and exploratory activity, a task thought to involve the hippocampus, was performed as established [49–52]. Y-maze is made up of dark gray acrylic material with three 21 cm-long arms, 4 cm wide, with walls a height of 40 cm (Accuscan Instruments, Inc.). Each animal received only one trial consisting of a 5-min duration in the Y-maze. Each animal was placed in the central zone intersected by all the three arms, and this entry location was kept consistent for all trials and for all animals in a given experimental group. The animal was allowed to explore freely in all three arms for the total duration of 5 min. Alterations and total number of arm-entries/choices were recorded with the use of CCD video camera (SONY) connected to the computer, and registered with the use of Accutrack software (AccuScan Inc., Columbus, OH). The animal was expected to explore and make more entries in all the three arms (A, B, C). Shorter time spent in each arm accompanied by higher frequency of entry in different arms indicated that the spontaneous exploratory activity involving hippocampus was not deteriorated. On the other hand, longer time spent in each arm with less frequent entry in all arms indicated disability in hippocampus-based spontaneous working memory. Since the animals were tested for “spontaneous” behavior, each animal was subjected to the Y-maze test only once. Spontaneous working memory for each animal was recorded and individual values used to derive a group mean and then analyzed.

Immunohistochemistry

Immunohistochemical analysis of synaptophysin, Aβ, and phospho-tau distribution in hippocampus was performed using Sternberger’s peroxidase-anti-peroxidase (PAP) technique as established [49, 51, 53–55]. Briefly, sections were deparaffinized, hydrated, endogenous peroxidase quenched in methanolic 0.6% H_2O_2 for 30 min at room temperature

(RT), and washed in the wash solution [10 mM Tris-HCl (pH 7.6), 0.5% bovine serum albumin and 0.87% NaCl], 3 times for 5 min each. After this step, all incubations will be performed in a humid chamber at RT. Sections were incubated with; (a) 5% non-immune host serum (in which the primary antibody is produced) for 60 min; (b) followed by optimal dilution of respective primary antibody [synaptophysin (MAB368, mouse monoclonal anti-synaptophysin antibody raised against ~38 kDa presynaptic vesicular protein, SVP-38 clone) (Millipore/Chemicon)], [Aβ (4G8, mouse monoclonal anti-Aβ antibody raised against 17–28 amino acid residues of Aβ) (Covance)], and [phospho-tau (AT8, mouse monoclonal anti-tau antibody that recognizing tau protein phosphorylated at serine 202 and threonine 205 phosphorylation epitope-sites of paired helical filament/PHF-tau protein) (Innogenetics)]; diluted with antibody dilution buffer [10 mM Tris-HCl (pH 7.6), 0.5% goat serum and 0.1% Triton X100], for 18–20 h; (c) washed in wash solution; goat anti-mouse/rabbit IgG optimally diluted with 1% goat serum for 60 min, and washed as in (c). Then the sections were incubated with optimal mouse/rabbit PAP complex diluted with antibody dilution buffer for 60 min, washed as in (c), and incubated in chromogenic solution [0.06% 3,3′-diaminobenzidine tetrahydrochloride, 0.01% H_2O_2 in 50 mM Tris-HCl (pH 7.6)] for 8 min to reveal HRP label. Chromogenic reaction was stopped by immersing sections in distilled water. The sections were dehydrated and mounted in Permount (Fisher Scientific). Procedural controls consisted of omission of primary antiserum (omit controls) and incubating sections with host-serum (serum controls).

Densitometric quantitation

Densitometric quantitation of 4G8-immunoreactivity (IR) Aβ and AT8-IR phospho-tau was performed within 200 $m\mu^2$ high power fields (hpfs) of CA1-3 (5 hpfs/unilaterally/bilateral hippocampi/section, 2 sections/animal), and dentate gyrus (DG) (5 hpfs/bilateral hippocampi/section, 2 sections/animal) hippocampal subfields of brain sections (Bregma −2.06–2.36). Quantitation of (SYN)-IR was performed within 100 $m\mu^2$ hpfs of CA3 (3 hpfs/unilaterally/bilateral hippocampi/section, 2 sections/animal); and within 100 $m\mu^2$ hpfs of supra-plus sub-granular layers DG (6 hpfs/unilaterally/bilateral hippocampi/section, 2 sections/animal) hippocampal subfields of brain sections (Bregma −2.06–2.36). These measurements were performed with the use of ImagePro and ImageJ programs loaded on Olympus BX41 series microscope and analyzed.

Enzyme-linked immunosorbent assay for cerebral Aβ

Quantitation of soluble (s) species of cerebral Aβ from HF- or LF-fed SAMP8 mice and HF- or LF-fed SAMPR1 mice was performed using ELISA as established [54–58]. An aliquot containing 100 μg/100μl protein was used to measure $sA\beta_{40}$ and $sA\beta_{42}$ (Covance), cytochrome c oxidase, and pyruvate dehydrogenase (Abcam.com) with the use of commercial kits. Values were expressed as pg/mg protein, and group means were analyzed.

Western blotting

GSK3β is a proline-directed serine/threonine protein kinase, is active when phosphorylated at its tyrosine 216 residue [GSK3β (Y216)-active form of GSK3β] by fyn kinase and inactivated when phosphorylated at its serine 9 residue [GSK3β (S9)-inactive form of GSK3β]. The active form of GSK3β is accounted for phosphorylating ~75% of paired helical filament (PHF)-tau [59, 60]. Therefore, although several kinases (other than GSK3β) are involved in phosphorylating tau protein, we chose to analyze GSK3β since it is the most prominent tau kinase in the brain [61–63] phosphorylating tau epitopes at almost more than twice as many sites in PHF-tau than the other kinases including mitogen activated protein kinase (MAPK)/extracellular signal regulated kinase 2, MAPK/-c-Jun N-terminal kinase, MAPK-p38 or cyclin-dependent kinase 5 [59, 60, 64–67]. Specifically, GSK3β is expected

to phosphorylate number of PHF-tau epitopes including serine (46, 198, 199, 202, 235, 262, 356, 396, 400, 413) and threonine (181, 205, 212, 217, 231, 403, 404) sites.

The IR for active and inactive forms of GSK3β were quantitated by western blot analysis of the brains from diabetic and non-diabetic SAMP8 and SAMPR1 mice as established [54–58]. Briefly, brains were homogenized in modified RIPA buffer containing protease/phosphatase inhibitors cocktail (Sigma), sonicated for 30 s, and centrifuged at 100,000 g for 1 h at 4° C. Supernatants were subjected to protein estimation (Pierce). Samples containing 50 μg of protein were electrophoresed on NuPage 4–12% Bis-Tris precast gels (Life Technologies) under reducing conditions using NuPage MES SDS Running Buffer (Life Technologies). Separated proteins were transferred on PVDF membranes. Membranes were washed and blocked with 5% dry milk in TBST, reacted with optimally diluted primary antisera raised against anti-Y216 GSK3β (BioSource, recognizing GSK3β phosphorylated at tyrosine 216 site-activated form of GSK3β), and raised against anti-S9 GSK3β (BioSource, recognizing GSK3β phosphorylated at serine 9 site-inactive form of GSK3β), washed and reacted with secondary HRP conjugated antibody, washed, developed with Electrochemiluminescence (ECL) (Pierce), and quantitated using Kodak X-5100R. Values were normalized with total GSK3β-IR.

Statistical analysis

Statistical analysis of the data was performed using GraphPad Prism Program. Data were analyzed to obtain group means with standard deviation (SD). The data were further subjected to omnibus analysis of variance (ANOVA) to determine if there is a main effect of the treatment across the groups, followed by Tukey posthoc test for comparisons between control and experimental groups. Morris water maze spatial learning data was analyzed by repeated measures analysis of variance (RMANOVA) followed by Tukey *post hoc* test. A value of $p < 0.05$ was considered statistically significant.

RESULTS

Development of experimental T2DM in SAMP8 and SAMPR1 mice

Feeding of HF exhibited exponential increase in body weight both in SAMP8 and SAMPR1 mice up to 12 weeks of HF feeding, in contrast to LF-fed mice at the parallel time-points. Consistent with previous reports [44], experimental induction of T2DM both in SAMP8 and SAMPR1 mice was evident at 8 weeks of HF feeding, as observed by time-dependent increase in fasting blood glucose levels, peaking at 8 weeks of HF feeding, parallel with gain in body weight, sustained up to 12 weeks. It was observed that the fasting blood glucose levels exponentially increased by 2.6–2.9-fold from week 1 up to12 weeks of HF feeding. Both in SAMP8 and SAMPR1 mice, insulin levels were increased by 8 weeks of HF feeding, sustained up to 12 weeks (Table 1).

Persistent high blood glucose levels between 20–90 min of glucose tolerance test at 8 and 12 weeks post HF treatment both in SAMP8 and SAMPR1 mice indicate systemic failure to reduce blood glucose indicating sustained pancreatic dysfunction due to insulin resistance by 8 weeks post-HF continued up to 12 weeks post-HF diet (Fig. 2). These results confirm that both SAMP8 and SAMPR1 mice developed insulin resistant T2DM by 8 weeks of HF treatment and that this condition was sustained up to 12 weeks post HF treatment.

Learning and memory deficits were further aggravated in diabetic SAMP8 mice

Aging-resistant non-diabetic SAMPR1 mice fed with LF control diet exhibited base-line spatial acquisition learning behavior with the latencies to reach the submerged platform ranging between 15-11 s from day1 through day3 learning trials (Fig. 2, open squares). This

performance was deteriorated by ↓1.4-fold ($p < 0.05$) in diabetic SAMPR1 mice fed with HF (Fig. 2, compare filled squares to open squares). When compared to LF-fed non-diabetic SAMPR1 mice, LF-fed non-diabetic SAMP8 mice exhibited ↓1.6-fold ($p < 0.05$) deterioration in spatial learning (Fig. 2, compare open squares to open circles). Diabetic SAMP8 mice fed with HF diet exhibited maximum deficits in spatial learning as evidenced by ↓1.4-fold ($p < 0.05$) deterioration compared to LF-fed non-diabetic SAMP8 mice (Fig. 2, compare filled circles to open circles); ↓1.6-fold deterioration ($p < 0.05$) compared to HF-fed diabetic SAMPR1 mice (Fig. 2, compare filled circles to filled squares); and maximum deterioration of ↓ 2.4-fold ($p < 0.0001$) compared to LF-fed non-diabetic SAMPR1 mice (Fig. 2, compare filled circles to open squares). Thus, diabetic SAMP8 mice showed maximally impaired spatial acquisition learning.

With regard to retention memory, however, the trend was slightly different in diabetic SAMPR1 mice versus non-diabetic SAMP8 mice. Aging-resistant non-diabetic SAMPR1 mice fed with LF control diet exhibited excellent retention memory profile with the most time (~53 s) spent in the quadrant that previously contained the submerged platform (PQ) (Fig. 3, PQ), and the least time (~7 s) spent in other quadrants (Fig. 3, Q1, Q2, Q3). Compared to non-diabetic SAMPR1 mice, retention memory was observed to be gradually deteriorated in LF-fed non-diabetic SAMP8 mice, that spent ~47 s in PQ [(↓ 1.16-fold, $p < 0.05$; SAMPR1-LF versus SAMP8-LF) (Fig. 3)]; with greater deterioration in HF-fed diabetic SAMPR1 mice, that spent ~38 s in PQ [(↓1.4-fold, $p < 0.05$; SAMPR1-LF versus SAMR1-HF) (Fig. 3)]; and with greatest deterioration in HF-fed diabetic SAMP8 mice, that spent only ~29 s in PQ [(↓ 2.2-fold, $p < 0.004$; SAMPR1-LF versus SAMP8-HF) (Fig. 3)]. Thus, diabetic SAMP8 mice showed maximally impaired retention memory. Thus, diabetic SAMP8 mice exhibited maximally impaired memory [↓ 1.4-fold ($p < 0.05$) versus non-diabetic SAMP8; ↓ 1.16-fold ($p < 0.05$) versus diabetic SAMPR1; ↓ 2.2-fold ($p < 0.004$) versus non-diabetic SAMPR1].

The reference working memory profile evaluated by spontaneous exploration using Y maze, in SAMP8 and SAMPR1 mice with and without diabetes was observed to be similar to the acquisition learning index. Aging-resistant non-diabetic SAMPR1 mice fed with LF exhibited preserved reference working memory showing maximum amount of exploration and alterations in all arms (~140 s) (Fig. 4, SAMPR1-LF), which was moderately impaired by ↓ 1.3-fold ($p < 0.05$) in diabetic SAMPR1 mice fed with HF showing relatively reduced amount of explorations and alterations (~107 s) (Fig. 4, SAMPR1-HF). Compared to LF-fed non-diabetic SAMPR1 mice, LF-fed non-diabetic SAMP8 mice exhibited ↓ 1.8-fold ($p < 0.05$) impairment in reference working memory (Fig. 4). Diabetic SAMP8 mice exhibited maximum working memory deficits as observed by ↓ 2.6-fold deterioration ($p < 0.003$) compared to non-diabetic SAMPR1 mice (Fig. 4). Thus, diabetic SAMP8 mice showed maximally impaired working reference memory. These results indicate that compared to "aging" alone, "diabetes" by itself was more effective in deteriorating retention memory; while compared to "diabetes" alone, "aging" by itself was more effective in deteriorating acquisition learning and spontaneous exploration; and that diabetic SAMP8 mice exhibited maximum deterioration in all behavioral tasks.

Superfluous elevation of cerebral amyloid in diabetic SAMP8 mice

ELISA profile of cerebral Aβ showed that the levels of $sA\beta_{40}$ and $sA\beta_{42}$ in SAMPR1 mice fed either with HF or with LF were not observed to be significantly different (Fig. 5). Levels of $sA\beta_{40}$ and $sA\beta_{42}$ in LF-fed SAMP8 mice were observed to ↑ 3.5-fold ($p < 0.003$) greater than those of HF-or LF-fed SAMPR1 mice indicating that the base levels of $sA\beta_{40}$ and $sA\beta_{42}$ in SAMP8 mice were greater than SAMPR1 mice (Fig. 5). HF treatment in SAMP8 mice significantly elevated levels of $sA\beta_{40}$ and $sA\beta_{42}$, both compared to LF-fed SAMP8

mice (↑ 3.5-fold, $p < 0.003$) and compared to HF- or LF-fed SAMPR1 mice (↑ 6.5-fold, $p < 0.0001$) (Fig. 5), indicating that diabetic SAMP8 mice showed most significantly increased levels of cerebral $sA\beta_{40}$ and $sA\beta_{42}$. Immunohistochemical profile of cerebral Aβ showed faint intraneuronal deposition of 4G8-IR Aβ in the brains of non-diabetic SAMP8 mice within the hippocampal neurons (Fig. 6A, inlet, arrowheads) but there was no parenchymal Aβ deposition (Fig. 6A). On the other hand, diabetic SAMP8 mice exhibited increased deposition of intraneuronal Aβ (Fig. 6B, inlet, arrowheads) as well as parenchymal deposition of Aβ (Fig. 6) in the hippocampus, indicating that HF-diet induced diabetic SAMP8 mice showed increased cerebral Aβ deposition both within the neurons and parenchyma, leaning toward Alzheimer-like changes. Densitometric quantitation confirmed the increase of 4G8-IR Aβ both in the CA1-3 and DG hippocampal subfields. LF-fed non-diabetic SAMPR1 mice showed base levels of 4G8-IR in the CA1-3 and DG hippocampal subfields which were increased by 1.8-fold ($p < 0.05$) in CA1-3, and increased by 2.0-fold ($p < 0.05$) in DG of both HF-fed diabetic SAMPR1 mice and LF-fed non-diabetic SAMP8 mice (Fig. 7). Compared to both HF-fed diabetic SAMPR1 mice and LF-fed non-diabetic SAMP8 mice, HF-fed diabetic SAMP8 mice exhibited maximum deposition of 4G8-IR Aβ (CA1-3, ↑ 1.7-fold, $p < 0.05$; DG, ↑ 2.2-fold, $p < 0.004$) (Fig. 7).

Evidence of tau phosphorylation in diabetic SAMP8 mice

Parallel to the exaggeration of cerebral amyloid, an increased trend of tau phosphorylation in diabetic SAMP8 mice was observed, as evidenced by increased IR of phospho-tau (AT8). Immunohistochemical index of phospho-tau (AT8) showed that there was a subtle deposition of AT8-IR in the hippocampal neuronal processes in the brains of non-diabetic SAMP8 mice (Fig. 6 C, inlet, arrowhead), which was found to increase in the hippocampal neuronal processes of diabetic SAMP8 mice (Fig. 6D, inlet, arrowheads) suggesting that HF-induced T2DM in SAMP8 mice promoted increased deposition of phospho-tau, a trend toward Alzheimer-like changes. Densitometric quantitation confirmed increased AT8-IR both in the CA1-3 and DG hippocampal subfields. LF-fed non-diabetic SAMPR1 mice showed base levels of AT8-IR in the CA1-3 and DG hippocampal subfields which were increased by 2.5-fold ($p < 0.005$) in CA1-3, and increased by 2.6-fold ($p < 0.005$) in DG of both HF-fed diabetic SAMPR1 mice and LF-fed non-diabetic SAMP8 mice (Fig. 7). Compared to both HF-fed diabetic SAMPR1 mice and LF-fed non-diabetic SAMP8 mice, HF-fed diabetic SAMP8 mice exhibited maximally increased AT8-IR (CA1-3, ↑ 1.4-fold, $p < 0.05$; DG, ↑ 1.5-fold, $p < 0.002$) (Fig. 7).

With regard to the profile of tau-phosphorylating enzyme GSK3β, it was observed that active form of GSK3β (Y216) was prominent in SAMP8 mice while inactive form of GSK3β (S9) was prominent in SAMPR1 mice regardless of HF or LF dietary treatments (Fig. 8). HF or LF dietary treatment did not alter the density of inactive GSK3β (S9) both in SAMP8 or SAMPR1 mice. Compared to LF-fed non-diabetic SAMP8 mice, HF treatment increased activated GSK3β (Y216) by ↑ 1.6-fold in SAMP8 mice ($p < 0.004$), but not in SAMPR1 mice (Fig. 8). Compared to HF/LF-fed SAMPR1 mice, activated GSK3β (Y216) is increased by ↑ 2.2-fold ($p < 0.0001$) in LF-fed, and by ↑ 3.5-fold ($p < 0.0001$) in HF-fed SAMP8 mice (Fig. 8). Results indicate that cerebral GSK3β was dysregulated only in diabetic SAMP8 mice, but not in diabetic SAMPR1 or non-diabetic SAMPR1 or SAMP8 mice.

Evidence of aggravated synaptic deficits in diabetic SAMP8 mice

Parallel to the exaggeration of cerebral amyloid and tau pathology, there was observed a marked synaptic deficit in diabetic SAMP8 mice as evidenced by selectively decreased IR of one of the presynaptic vesicular markers-synaptophysin (SYN), in the hippocampus of diabetic SAMP8 mice. As evidenced in Fig. 9, LF-fed non-diabetic SAMPR1 mice showed

prominent SYN-IR within the hippocampal CA3 dendritic field (Fig. 9A, black arrow) and within the supra-granular (Fig. 9A, black arrowhead) and sub-granular (Fig. 9A, white arrowhead) molecular layers of DG. Feeding HF to SAMPR1 mice decreased SYN-IR within the respective hippocampal dendritic fields (compare black arrow, black arrowhead, and white arrowhead in Fig. 9B to 9A). Interestingly, the base levels of SYN-IR within the respective hippocampal dendritic fields of the LF-fed non-diabetic SAMP8 mice were very much similar to those observed for diabetic SAMPR1 mice (compare black arrow, black arrowhead, and white arrowhead in Fig. 9C to 9B). Experimental induction of T2DM after feeding HF to SAMP8 mice, remarkably reduced SYN-IR within the respective hippocampal dendritic fields of diabetic SAMP8 mice (compare black arrow, black arrowhead, and white arrowhead in Fig. 9D to 9C), indicating that SYN-IR was drastically reduced in diabetic SAMP8 mice.

Densitometric quantitation showed decreased SYN-IR both in the CA3 and DG hippocampal subfields. LF-fed non-diabetic SAMPR1 mice showed base levels of SYN-IR in the CA3 and DG hippocampal subfields which were decreased by 1.4-fold ($p < 0.05$) in CA3, and decreased by 1.3-fold ($p < 0.05$) in DG of both HF-fed diabetic SAMPR1 mice and LF-fed non-diabetic SAMP8 mice (Fig. 10). Compared to both HF-fed diabetic SAMPR1 mice and LF-fed non-diabetic SAMP8 mice, HF-fed diabetic SAMP8 mice exhibited maximally decreased SYN-IR (CA3, ↓ 1.8-fold, $p < 0.004$; DG, ↓ 2.0-fold, $p < 0.005$) (Fig. 10). These observations show that although HF-induced T2DM affected both CA3 and DG with regard to the depletion of SYN-IR, CA3 was relatively more affected than DG. In summary, diabetic SAMP8 mice exhibited Alzheimer-like neuropathological and cognitive signs.

DISCUSSION

Current investigation emphasizes the role of diabetes as a non-familial co-morbid factor in producing Alzheimer-like characteristics when combined with accelerated aging. This current study clearly showed aggravating effects of insulin dysfunction even after a shortly sustained experimental T2DM on the development of early Alzheimer-like neuropathological and cognitive impairments, indicating that further sustainment of T2DM in SAMP8 mice has a potential to develop characteristic features typifying the disease.

Insulin deficiency and/or inability of neurons to respond to insulin-stimulus (insulin resistance) is known to impair neuronal functions at several levels based on emerging evidence indicating its importance in the functioning of the brain, besides its known glucoregulatory and growth promoting effects in the periphery [68–70]. Expression of insulin receptors throughout the brain [71], with relative greater abundance in hippocampus, cortex, and amygdala (the brain regions critically involved in AD [69, 71]), support a significant role played by insulin and its signaling in AD. Approximately 50% of brain and body growth is mediated by the insulin-insulin growth factor (IGF) signaling system [72, 73]. Most of the brain insulin is derived from periphery and is taken up by the brain via a receptor-uptake mechanism [74, 75]. Insulin exerts pleiotropic effects in neurons including regulation of neural proliferation, apoptosis, and synaptic transmission [14, 24, 76]. Insulin and IGF-1 are neurotrophic that support neuronal growth, survival, differentiation, outgrowth, migration, neuronal cytoskeleton, protein synthesis, and synapse formation [71]. Insulin signaling plays a role in synaptic plasticity by modulating activities of excitatory and inhibitory receptors such as glutamate and GABA receptors, and by triggering signal transduction cascade leading to the alteration of gene expression required for long term memory [69, 77–79]. Thus, either insulin deficiency or inability of neurons to respond to insulin-stimulus (insulin resistance) may impair neuronal functions at several levels.

While insulin is neurotrophic at optimum concentration, too much insulin in the brain resulting from insulin resistance may be associated with reduced Aβ clearance since both insulin and Aβ compete for the availability of insulin degrading enzyme, and since insulin degrading enzyme is much more selective for insulin than Aβ [17]. Besides an impaired energy balance in the brain cells due to altered glucose metabolism [4, 26], high prevalence of insulin resistance/hyperinsulinemia [9, 12, 13, 15, 16, 27] restricts the Aβ degrading ability of insulin degrading enzyme [28] and glucagon-like peptide-1 [29]. Insulin has been shown to upregulate AβPP mRNA expression [30] and reduce cytotoxicity induced by Aβ in a dose-dependent manner [80]. Insulin is known to hamper Aβ production via modulation of α-secretase activity and Aβ degradation [81], while insulin resistance is reported to promote Aβ build up in the brain via altered insulin signal transduction, increased β-secretase and β-secretase activities, and accumulation of autophagosomes involved in the release of Aβ [82]. Moreover, brain insulin resistance accelerates Aβ fibrillogenesis via induction of GM1 ganglioside [83]. On the other hand, increased Aβ prompts the onset of glucose intolerance and insulin resistance [84], setting up a vicious feed-back loop of Aβ and insulin resistance.

Currently observed increases in the levels of soluble $A\beta_{40}$ and $A\beta_{42}$ measured by ELISA and faint perikaryal 4G8 immunolocalization in the hippocampal neurons of non-diabetic SAMP8 mice may be attributed to the amyloidogenic effects of accelerated brain aging. However, greater increases in the levels of soluble $A\beta_{40}$ and $A\beta_{42}$ measured by ELISA and increased deposition of 4G8-positive Aβ in the hippocampus of diabetic SAMP8 mice, compared to those of non-diabetic SAMP8 mice, certainly appears to be accentuated due to HF-induced sustained diabetes, which consistently corroborates with the reported amyloidogenic effects of insulin resistance in the brain [80].

Current data implicate that although “aging” by itself promotes Aβ production, “aging” alone is not sufficient to aggravate pathological accumulation of Aβ, unless accompanied with other comorbid factor(s)-such as insulin dysfunction. Aging alone is known to elevate oxidative damage and inflammation [85, 86]. On the other hand, diabetes by itself is known to produce inflammation and oxidative damage [87–90]. Therefore, when “aging” and “diabetes” are combined, chronic oxidative damage [91, 92] and neuroinflammation [93, 94], independently resulting from aging and diabetes, lead to “exacerbation” of Aβ production. Moreover, diabetes is known to reduce Aβ clearance [17, 95] and speed up Aβ fibrillogenesis via GM1 ganglioside [83], adding to the accumulation of Aβ. Aβ in turn is known to make the neurons resistant to insulin [95, 96], thus setting up a vicious interplay of Aβ and insulin resistance. Based on these facts, Aβ cascade does exist; however, compounded consequences of aging and diabetes make it worst. Oxidative damage and neuroinflammation in aging brain and diabetes appear to reside upstream of exaggerated production and accumulation of Aβ. Consistent with experimental and clinical reports [87, 96–100], current data show that diabetes “adds” to the oxidative and inflammatory effects produced by aging, and sets up a vicious interplay of Aβ and insulin resistance and impaired insulin signaling.

In addition to the amyloidogenic effects of insulin dysfunction, experimental evidence also suggests its role in promoting synaptic and cognitive deficits. Mice with systemic insulin deficiency display an evidence of reduced insulin signaling in the brain that is associated with synaptic and behavioral features of AD [15]. T2DM associated with insulin resistance show reduced insulin brain uptake and content, suggesting that brain insulin receptors become less sensitive to insulin, which could reduce synaptic plasticity [74]. Impaired insulin signaling is shown to decrease the trafficking and function of postsynaptic glutamate receptors leading synaptic deficits and memory loss [34]. Since insulin acts as a “neuromodulator”, it may influence release and re-uptake of neurotransmitters improving memory [97] and promote dendritic spine formation and excitatory synapse development

[101]. Thus, insulin dysfunction may lead to synaptic and cognitive deficits [102]. Supporting evidence in this regard indicates that brain depletion of insulin receptor substrate 2 disrupts hippocampal synaptic plasticity [103]. In HF-fat fed diabetic mice, significant impairment in hippocampal long term potentiation is observed [104], and decreased spontaneous alteration in Y maze accompanied by decreased density of synaptophysin and SNAP25 nerve terminal markers are observed [105].

Consistent with these reports, our data show that while a LF diet maintained strong synaptophysin immunoreactivity within the hippocampal CA3 dendritic field as well as within the supra-granular and sub-granular molecular layers of DG of SAMPR1 mice, development of diabetes resulted in the reduction of synaptophysin immunoreactivity only in the CA3 dendritic field that receives inputs from entorhinal cortical perforant pathway, while preserving synaptophysin immunoreactivity within the supra-granular and sub-granular molecular layers of dentate gyrus, that project to the CA3 via mossy fiber connections. Since CA3 hippocampal sub-region is essential for the consolidation and retrieval of spatial memory, observed depletion of synaptophysin immunoreactivity in the CA3 subfield would indicate that independent of “aging”, diabetes alone may affect memory retrieval. In that regard, it is interesting to note that HF-fed diabetic SAMPR1 mice exhibited worsened retention memory than the non-diabetic SAMP8 mice.

By contrast, preserved synaptophysin immunoreactivity in the CA3 dendritic field, but depletion of synaptophysin immunoreactivity within the supra-granular and sub-granular molecular layers of DG in non-diabetic SAMP8 mice, indicate that “aging alone” in absence of diabetes may not disrupt consolidation and retrieval of spatial memory, but may impair the formation of new memories (learning or exploration). Consistent with this theory, current results confirm greater deterioration of learning and spontaneous exploration non-diabetic SAMP8 mice than those of diabetic SAMPR1 mice. Combining accelerated aging with diabetes exhibited depletion of synaptophysin immunoreactivity both in the CA3 dendritic fields and within the supra-granular and sub-granular molecular layers of DG, which was reflected in the drastic deterioration of learning, memory, and spontaneous exploration.

With regard to tau biology, insulin deficiency has been shown to promote pathological phosphorylation of tau in various models of insulin dysfunction. Tau has been found to be phosphorylated at multiple sites in mouse brain after streptozotocin-induced insulin deficiency [25, 106]. Alteration in GSK3β and deficits in hippocampal synaptic transmission with parallel deficits in hippocampal long term potentiation has been observed in streptozotocin-injected rodents [34]. Consistent with these earlier reports, abundant expression of activated form of GSK3β in diabetic SAMP8 mice actively involved in tau phosphorylation indicate that the index of tau phosphorylation is quite pronounced when aging and diabetic conditions are combined. As a matter of fact, these mice also showed structured “tangle-like” inclusions within the hippocampal neuronal processes as compared to the non-diabetic SAMP8 mice. Thus, the tau-phosphorylation pro-file seems to run in parallel with other degenerative changes and cognitive decline observed in diabetic SAMP8 mice.

CONCLUSIONS

Taken together, current study reinstates the role played by T2DM in potentiating Alzheimer-like patho-cognition when combined with accelerated aging, as evaluated by experimental induction of T2DM in aging accelerated SAMP8 mice. Depending upon the duration of T2DM sustainment, this model system has the utility to be exploited either as early-stage or late-stage sporadic AD. This research has great potential to maximize the understanding of

changes in the physiology and function of aging brain in presence of diabetes to determine the onset and progression of neurodegeneration, and bridge an important gap between molecular mechanisms and clinical therapeutics of AD. Our current study provides a pertinent model system to identify early interventional therapeutic targets and test candidate therapies during the early stage(s) of AD.

Acknowledgments

This material is the result of work supported with resources and the use of facilities at the Jesse Brown VA Medical Center, Chicago, IL. The authors acknowledge the support provided by the Westside Institute for Science and Education and by the Department of Pediatrics, University of Illinois at Chicago, Children's Hospital of the University of Illinois, Chicago, IL. This work has been supported in part by the National Institute of Health (AG039625, NS079614, NBC) and Department of Veterans Affairs, Veterans Health Administration, Office of Research and Development, Rehabilitation R&D (B6285R, I0880R, NBC).

References

1. Finder VH. Alzheimer's disease: A general introduction and pathomechanism. J Alzheimers Dis. 2010; 22(Suppl 3):5–19. [PubMed: 20858960]
2. Duyckaerts C, Delatour B, Potier MC. Classification and basic pathology of Alzheimer disease. Acta Neuropathol. 2009; 118:5–36. [PubMed: 19381658]
3. Bastos Leite AJ, Scheltens P, Barkhof F. Pathological aging of the brain: An overview. Top Magn Reson Imaging. 2004; 15:369–389. [PubMed: 16041289]
4. Craft S. The role of metabolic disorders in Alzheimer disease and vascular dementia: Two roads converged. Arch Neurol. 2009; 66:300–305. [PubMed: 19273747]
5. Luchsinger JA. Diabetes, related conditions, and dementia. J Neurol Sci. 2010; 299:35–38. [PubMed: 20888602]
6. Bhat NR. Linking cardiometabolic disorders to sporadic Alzheimer's disease: A perspective on potential mechanisms and mediators. J Neurochem. 2010; 115:551–562. [PubMed: 20807313]
7. Salkovic-Petrisic M, Hoyer S. Central insulin resistance as a trigger for sporadic Alzheimer-like pathology: An experimental approach. J Neural Transm Suppl. 2007:217–233. [PubMed: 17982898]
8. Jones A, Kulozik P, Ostertag A, Herzig S. Common pathological processes and transcriptional pathways in Alzheimer's disease and type 2 diabetes. J Alzheimers Dis. 2009; 16:787–808. [PubMed: 19387113]
9. Ronnemaa E, Zethelius B, Sundelof J, Sundstrom J, Degerman-Gunnarsson M, Berne C, Lannfelt L, Kilander L. Impaired insulin secretion increases the risk of Alzheimer disease. Neurology. 2008; 71:1065–1071. [PubMed: 18401020]
10. Currais A, Prior M, Lo D, Jolivalt C, Schubert D, Maher P. Diabetes exacerbates amyloid and neurovascular pathology in aging-accelerated mice. Aging Cell. 2012; 11:1017–1026. [PubMed: 22938075]
11. Burdo JR, Chen Q, Calcutt NA, Schubert D. The pathological interaction between diabetes and presymptomatic Alzheimer's disease. Neurobiol Aging. 2009; 30:1910–1917. [PubMed: 18372080]
12. Hoyer S. The aging brain. Changes in the neuronal insulin/insulin receptor signal transduction cascade trigger late-onset sporadic Alzheimer disease (SAD). A mini-review. J Neural Transm. 2002; 109:991–1002. [PubMed: 12111436]
13. Gasparini L, Xu H. Potential roles of insulin and IGF-1 in Alzheimer's disease. Trends Neurosci. 2003; 26:404–406. [PubMed: 12900169]
14. Sabayan B, Foroughinia F, Mowla A, Borhanihaghighi A. Role of insulin metabolism disturbances in the development of Alzheimer disease: Mini review. Am J Alzheimers Dis Other Demen. 2008; 23:192–199. [PubMed: 18198237]
15. Jolivalt CG, Lee CA, Beiswenger KK, Smith JL, Orlov M, Torrance MA, Masliah E. Defective insulin signaling pathway and increased glycogen synthase kinase-3 activity in the brain of

diabetic mice: Parallels with Alzheimer's disease and correction by insulin. J Neurosci Res. 2008; 86:3265–3274. [PubMed: 18627032]

16. Cukierman-Yaffee T. The relationship between dysglycemia and cognitive dysfunction. Curr Opin Investig Drugs. 2009; 10:70–74.
17. JSR-F, Sa-Roriz TM, Rosset I, Camozzato AL, Santos AC, Chaves ML, Moriguti JC, Roriz-Cruz M. (Pre)diabetes, brain aging, and cognition. Biochim Biophys Acta. 2009; 1792:432–443. [PubMed: 19135149]
18. Freude S, Schilbach K, Schubert M. The role of IGF-1 receptor and insulin receptor signaling for the pathogenesis of Alzheimer's disease: From model organisms to human disease. Curr Alzheimer Res. 2009; 6:213–223. [PubMed: 19519303]
19. de la Monte SM, Longato L, Tong M, Wands JR. Insulin resistance and neurodegeneration: Roles of obesity, type 2 diabetes mellitus and non-alcoholic steatohepatitis. Curr Opin Investig Drugs. 2009; 10:1049–1060.
20. Steen E, Terry BM, Rivera EJ, Cannon JL, Neely TR, Tavares R, Xu XJ, Wands JR, de la Monte SM. Impaired insulin and insulin-like growth factor expression and signaling mechanisms in Alzheimer's disease–is this type 3 diabetes? J Alzheimers Dis. 2005; 7:63–80. [PubMed: 15750215]
21. de la Monte SM, Neusner A, Chu J, Lawton M. Epidemilogical trends strongly suggest exposures as etiologic agents in the pathogenesis of sporadic Alzheimer's disease, diabetes mellitus, and non-alcoholic steatohepatitis. J Alzheimers Dis. 2009; 17:519–529. [PubMed: 19363256]
22. Kroner Z. The relationship between Alzheimer's disease and diabetes: Type 3 diabetes? Altern Med Rev. 2009; 14:373–379. [PubMed: 20030463]
23. Zhao WQ, Townsend M. Insulin resistance and amyloidogenesis as common molecular foundation for type 2 diabetes and Alzheimer's disease. Biochim Biophys Acta. 2009; 1792:482–496. [PubMed: 19026743]
24. Cole GM, Frautschy SA. The role of insulin and neurotrophic factor signaling in brain aging and Alzheimer's disease. Exp Gerontol. 2007; 42:10–21. [PubMed: 17049785]
25. Clodfelder-Miller BJ, Zmijewska AA, Johnson GV, Jope RS. Tau is hyperphosphorylated at multiple sites in mouse brain *in vivo* after streptozotocin-induced insulin deficiency. Diabetes. 2006; 55:3320–3325. [PubMed: 17130475]
26. Convit A, Wolf OT, Tarshish C, de Leon MJ. Reduced glucose tolerance is associated with poor memory performance and hippocampal atrophy among normal elderly. Proc Natl Acad Sci U S A. 2003; 100:2019–2022. [PubMed: 12571363]
27. Xu WL, von Strauss E, Qiu CX, Winblad B, Fratiglioni L. Uncontrolled diabetes increases the risk of Alzheimer's disease: A population-based cohort study. Diabetologia. 2009; 52:1031–1039. [PubMed: 19280172]
28. Cook DG, Leverenz JB, McMillan PJ, Kulstad JJ, Ericksen S, Roth RA, Schellenberg GD, Jin LW, Kovacina KS, Craft S. Reduced hippocampal insulin-degrading enzyme in late-onset Alzheimer's disease is associated with the apolipoprotein E-epsilon4 allele. Am J Pathol. 2003; 162:313–319. [PubMed: 12507914]
29. Li Y, Duffy KB, Ottinger MA, Ray B, Bailey JA, Holloway HW, Tweedie D, Perry T, Mattson MP, Kapogiannis D, Sambamurti K, Lahiri DK, Greig NH. GLP-1 receptor stimulation reduces amyloid-beta peptide accumulation and cytotoxicity in cellular and animal models of Alzheimer's disease. J Alzheimers Dis. 2010; 19:1205–1219. [PubMed: 20308787]
30. Lee YH, Tharp WG, Maple RL, Nair S, Permana PA, Pratley RE. Amyloid precursor protein expression is upregulated in adipocytes in obesity. Obesity (Silver Spring). 2008; 16:1493–1500. [PubMed: 18483477]
31. Zhao WQ, Lacor PN, Chen H, Lambert MP, Quon MJ, Krafft GA, Klein WL. Insulin receptor dysfunction impairs cellular clearance of neurotoxic oligomeric a{beta}. J Biol Chem. 2009; 284:18742–18753. [PubMed: 19406747]
32. Stranahan AM, Norman ED, Lee K, Cutler RG, Telljohann RS, Egan JM, Mattson MP. Diet-induced insulin resistance impairs hippocampal synaptic plasticity and cognition in middle-aged rats. Hippocampus. 2008; 18:1085–1088. [PubMed: 18651634]

33. Wang P, Jiang S, Cui Y, Yue Z, Su C, Sun J, Sheng S, Tian J. The n-terminal 5-MER peptide analogue P165 of amyloid precursor protein exerts protective effects on SH-SY5Y cells and rat hippocampus neuronal synapses. Neuroscience. 2011; 173:169–178. [PubMed: 21055450]
34. Shonesy BC, Thiruchelvam K, Parameshwaran K, Rahman EA, Karuppagounder SS, Huggins KW, Pinkert CA, Amin R, Dhanasekaran M, Suppiramaniam V. Central insulin resistance and synaptic dysfunction in intracerebroventricular-streptozotocin injected rodents. Neurobiol Aging. 2012; 33:430 e435–418. [PubMed: 21256630]
35. Lu FP, Lin KP, Kuo HK. Diabetes and the risk of multi-system aging phenotypes: A systematic review and meta-analysis. PLoS One. 2009; 4:e4144. [PubMed: 19127292]
36. Barrou Z, Lemaire A, Boddaert J, Verny M. Diabetes mellitus and cognition: Is there a link? Psychol Neuropsychiatr Vieil. 2008; 6:189–198. [PubMed: 18786878]
37. Moroz N, Tong M, Longato L, Xu H, de la Monte SM. Limited Alzheimer-type neurodegeneration in experimental obesity and type 2 diabetes mellitus. J Alzheimers Dis. 2008; 15:29–44. [PubMed: 18780965]
38. Takeda S, Sato N, Uchio-Yamada K, Sawada K, Kunieda T, Takeuchi D, Kurinami H, Shinohara M, Rakugi H, Morishita R. Diabetes-accelerated memory dysfunction via cerebrovascular inflammation and Abeta deposition in an Alzheimer mouse model with diabetes. Proc Natl Acad Sci U S A. 2010; 107:7036–7041. [PubMed: 20231468]
39. Torres-Aleman I. Mouse models of Alzheimer's dementia: Current concepts and new trends. Endocrinology. 2008; 149:5952–5957. [PubMed: 18818286]
40. Woodruff-Pak DS. Animal models of Alzheimer's disease: Therapeutic implications. J Alzheimers Dis. 2008; 15:507–521. [PubMed: 19096153]
41. Butterfield DA, Poon HF. The senescence-accelerated prone mouse (SAMP8): A model of age-related cognitive decline with relevance to alterations of the gene expression and protein abnormalities in Alzheimer's disease. Exp Gerontol. 2005; 40:774–783. [PubMed: 16026957]
42. Pallas M, Camins A, Smith MA, Perry G, Lee HG, Casadesus G. From aging to Alzheimer's disease: Unveiling "the switch" with the senescence-accelerated mouse model (SAMP8). J Alzheimers Dis. 2008; 15:615–624. [PubMed: 19096160]
43. Takeda T. Senescence-accelerated mouse (SAM) with special references to neurodegeneration models, SAMP8 and SAMP10 mice. Neurochem Res. 2009; 34:639–659. [PubMed: 19199030]
44. Rossmeisl M, Rim JS, Koza RA, Kozak LP. Variation in type 2 diabetes–related traits in mouse strains susceptible to diet-induced obesity. Diabetes. 2003; 52:1958–1966. [PubMed: 12882911]
45. Karasawa H, Nagata-Goto S, Takaishi K, Kumagae Y. A novel model of type 2 diabetes mellitus based on obesity induced by high-fat diet in BDF1 mice. Metabolism. 2009; 58:296–303. [PubMed: 19217442]
46. Sullivan KA, Lentz SI, Roberts JL Jr, Feldman EL. Criteria for creating and assessing mouse models of diabetic neuropathy. Curr Drug Targets. 2008; 9:3–13. [PubMed: 18220709]
47. Russell JC, Proctor SD. Small animal models of cardiovascular disease: Tools for the study of the roles of metabolic syndrome, dyslipidemia, and atherosclerosis. Cardiovasc Pathol. 2006; 15:318–330. [PubMed: 17113010]
48. Sandu O, Song K, Cai W, Zheng F, Uribarri J, Vlassara H. Insulin resistance and type 2 diabetes in high-fat-fed mice are linked to high glycotoxin intake. Diabetes. 2005; 54:2314–2319. [PubMed: 16046296]
49. Chauhan NB, Sandoval J. Amelioration of early cognitive deficits by aged garlic extract in Alzheimer's transgenic mice. Phytother Res. 2007; 21:629–640. [PubMed: 17380553]
50. Chauhan NB, Gatto R, Chauhan MB. Neuroanatom-ical correlation of behavioral deficits in the CCI model of TBI. J Neurosci Methods. 2010; 190:1–9. [PubMed: 20385166]
51. Chauhan NB, Gatto R. Synergistic benefits of erythropoietin and simvastatin after traumatic brain injury. Brain Res. 2010; 1360:177–192. [PubMed: 20833152]
52. Chauhan NB, Gatto R. Restoration of cognitive deficits after statin feeding in TBI. Restor Neurol Neurosci. 2011; 29:23–34. [PubMed: 21335666]
53. Chauhan NB. Intracerebroventricular passive immunization with anti-oligoAbeta antibody in TgCRND8. J Neurosci Res. 2007; 85:451–463. [PubMed: 17086547]

54. Chauhan NB, Siegel GJ. Antisense inhibition at the beta-secretase-site of beta-amyloid precursor protein reduces cerebral amyloid and acetyl cholinesterase activity in Tg2576. Neuroscience. 2007; 146:143–151. [PubMed: 17303345]
55. Ray B, Chauhan NB, Lahiri DK. Oxidative insults to neurons and synapse are prevented by aged garlic extract and S-allyl-l-cysteine treatment in the neuronal culture and APP-Tg mouse model. J Neurochem. 2011; 117:388–402. [PubMed: 21166677]
56. Chauhan NB, Siegel GJ, Feinstein DL. Effects of lovastatin and pravastatin on amyloid processing and inflammatory response in TgCRND8 brain. Neurochem Res. 2004; 29:1897–1911. [PubMed: 15532546]
57. Chauhan NB, Siegel GJ, Feinstein DL. Propento-fylline attenuates tau hyperphosphorylation in Alzheimer's Swedish mutant model Tg2576. Neuropharmacology. 2005; 48:93–104. [PubMed: 15617731]
58. Chauhan NB. Effect of aged garlic extract on APP processing and tau phosphorylation in Alzheimer's transgenic model Tg2576. J Ethnopharmacol. 2006; 108:385–394. [PubMed: 16842945]
59. Tomidokoro Y, Harigaya Y, Matsubara E, Ikeda M, Kawarabayashi T, Shirao T, Ishiguro K, Okamoto K, Younkin SG, Shoji M. Brain Abeta amyloidosis in APPsw mice induces accumulation of presenilin-1 and tau. J Pathol. 2001; 194:500–506. [PubMed: 11523060]
60. Tomidokoro Y, Ishiguro K, Harigaya Y, Matsubara E, Ikeda M, Park JM, Yasutake K, Kawarabayashi T, Okamoto K, Shoji M. Abeta amyloidosis induces the initial stage of tau accumulation in APP(Sw) mice. Neurosci Lett. 2001; 299:169–172. [PubMed: 11165762]
61. Jope RS, Johnson GV. The glamour and gloom of glycogen synthase kinase-3. Trends Biochem Sci. 2004; 29:95–102. [PubMed: 15102436]
62. Doble BW, Woodgett JR. GSK-3: Tricks of the trade for a multi-tasking kinase. J Cell Sci. 2003; 116:1175–1186. [PubMed: 12615961]
63. Sato S, Tatebayashi Y, Akagi T, Chui DH, Murayama M, Miyasaka T, Planel E, Tanemura K, Sun X, Hashikawa T, Yoshioka K, Ishiguro K, Takashima A. Aberrant tau phosphorylation by glycogen synthase kinase-3beta and JNK3 induces oligomeric tau fibrils in COS-7 cells. J Biol Chem. 2002; 277:42060–42065. [PubMed: 12191990]
64. Liu F, Iqbal K, Grundke-Iqbal I, Gong CX. Involvement of aberrant glycosylation in phosphorylation of tau by cdk5 and GSK-3beta. FEBS Lett. 2002; 530:209–214. [PubMed: 12387894]
65. Elyaman W, Yardin C, Hugon J. Involvement of glycogen synthase kinase-3beta and tau phosphorylation in neuronal Golgi disassembly. J Neurochem. 2002; 81:870–880. [PubMed: 12065646]
66. Reynolds CH, Betts JC, Blackstock WP, Nebreda AR, Anderton BH. Phosphorylation sites on tau identified by nanoelectrospray mass spectrometry: Differences *in vitro* between the mitogen-activated protein kinases ERK2, c-Jun N-terminal kinase and P38, and glycogen synthase kinase-3beta. J Neurochem. 2000; 74:1587–1595. [PubMed: 10737616]
67. Sperber BR, Leight S, Goedert M, Lee VM. Glycogen synthase kinase-3 beta phosphorylates tau protein at multiple sites in intact cells. Neurosci Lett. 1995; 197:149–153. [PubMed: 8552282]
68. Carro E, Torres-Aleman I. The role of insulin and insulin-like growth factor I in the molecular and cellular mechanisms underlying the pathology of Alzheimer's disease. Eur J Pharmacol. 2004; 490:127–133. [PubMed: 15094079]
69. Zhao WQ, Chen H, Quon MJ, Alkon DL. Insulin and the insulin receptor in experimental models of learning and memory. Eur J Pharmacol. 2004; 490:71–81. [PubMed: 15094074]
70. van der Heide LP, Ramakers GM, Smidt MP. Insulin signaling in the central nervous system: Learning to survive. Prog Neurobiol. 2006; 79:205–221. [PubMed: 16916571]
71. de la Monte SM, Wands JR. Review of insulin and insulin-like growth factor expression, signaling, and malfunction in the central nervous system: Relevance to Alzheimer's disease. J Alzheimers Dis. 2005; 7:45–61. [PubMed: 15750214]
72. Schubert M, Brazil DP, Burks DJ, Kushner JA, Ye J, Flint CL, Farhang-Fallah J, Dikkes P, Warot XM, Rio C, Corfas G, White MF. Insulin receptor substrate-2 deficiency impairs brain growth and promotes tau phosphorylation. J Neurosci. 2003; 23:7084–7092. [PubMed: 12904469]

73. Chiu SL, Cline HT. Insulin receptor signaling in the development of neuronal structure and function. Neural Dev. 2010; 5:7. [PubMed: 20230616]
74. Messier C, Teutenberg K. The role of insulin, insulin growth factor, and insulin-degrading enzyme in brain aging and Alzheimer's disease. Neural Plast. 2005; 12:311–328. [PubMed: 16444902]
75. Laron Z. Insulin and the brain. Arch Physiol Biochem. 2009; 115:112–116. [PubMed: 19485707]
76. Holscher C. The role of GLP-1 in neuronal activity and neurodegeneration. Vitam Horm. 2010; 84:331–354. [PubMed: 21094907]
77. Biessels GJ, Kappelle LJ. Increased risk of Alzheimer's disease in Type II diabetes: Insulin resistance of the brain or insulin-induced amyloid pathology? Biochem Soc Trans. 2005; 33:1041–1044. [PubMed: 16246041]
78. Huang CC, Lee CC, Hsu KS. The role of insulin receptor signaling in synaptic plasticity and cognitive function. Chang Gung Med J. 2010; 33:115–125. [PubMed: 20438663]
79. Nelson TJ, Sun MK, Hongpaisan J, Alkon DL. Insulin, PKC signaling pathways and synaptic remodeling during memory storage and neuronal repair. Eur J Pharmacol. 2008; 585:76–87. [PubMed: 18402935]
80. Di Carlo M, Picone P, Carrotta R, Giacomazza D, San Biagio PL. Insulin promotes survival of amyloid-beta oligomers neuroblastoma damaged cells via caspase 9 inhibition and Hsp70 upregulation. J Biomed Biotechnol. 2010; 2010:1–8.
81. Kojro E, Postina R. Regulated proteolysis of RAGE and AbetaPP as possible link between type 2 diabetes mellitus and Alzheimer's disease. J Alzheimers Dis. 2009; 16:865–878. [PubMed: 19387119]
82. Son SM, Song H, Byun J, Park KS, Jang HC, Park YJ, Mook-Jung I. Accumulation of autophagosomes contributes to enhanced amyloidogenic APP processing under insulin-resistant conditions. Autophagy. 2012; 8:1842–1844. [PubMed: 22931791]
83. Yamamoto N, Matsubara T, Sobue K, Tanida M, Kasahara R, Naruse K, Taniura H, Sato T, Suzuki K. Brain insulin resistance accelerates Abeta fibrillogenesis by inducing GM1 ganglioside clustering in the presynaptic membranes. J Neurochem. 2012; 121:619–628. [PubMed: 22260232]
84. Jimenez-Palomares M, Ramos-Rodriguez JJ, Lopez-Acosta JF, Pacheco-Herrero M, Lechuga-Sancho AM, Perdomo G, Garcia-Alloza M, Cozar-Castellano I. Increased Abeta production prompts the onset of glucose intolerance and insulin resistance. Am J Physiol Endocrinol Metab. 2012; 302:E1373–E1380. [PubMed: 22414803]
85. Jenny NS. Inflammation in aging: Cause, effect, or both? Discov Med. 2012; 13:451–460. [PubMed: 22742651]
86. Tilstra JS, Clauson CL, Niedernhofer LJ, Robbins PD. NF-kappaB in aging and disease. Aging Dis. 2011; 2:449–465. [PubMed: 22396894]
87. Hopps E, Caimi G. Protein oxidation in metabolic syndrome. Clin Invest Med. 2013; 36:E1–E8. [PubMed: 23374595]
88. Cai D. Neuroinflammation and neurodegeneration in overnutrition-induced diseases. Trends Endocrinol Metab. 2013; 24:40–47. [PubMed: 23265946]
89. Holscher C. Potential role of glucagon-like peptide-1 (GLP-1) in neuroprotection. CNS Drugs. 2012; 26:871–882. [PubMed: 22938097]
90. Johnson AR, Milner JJ, Makowski L. The inflammation highway: Metabolism accelerates inflammatory traffic in obesity. Immunol Rev. 2012; 249:218–238. [PubMed: 22889225]
91. Frautschy SA, Cole GM. Why pleiotropic interventions are needed for Alzheimer's disease. Mol Neurobiol. 2010; 41:392–409. [PubMed: 20437209]
92. Mohsenzadegan M, Mirshafiey A. The immunopathogenic role of reactive oxygen species in Alzheimer disease. Iran J Allergy Asthma Immunol. 2012; 11:203–216. [PubMed: 22947905]
93. Sutinen EM, Pirttila T, Anderson G, Salminen A, Ojala JO. Pro-inflammatory interleukin-18 increases Alzheimer's disease-associated amyloid-beta production in human neuron-like cells. J Neuroinflammation. 2012; 9:199. [PubMed: 22898493]
94. Chakrabarty P, Tianbai L, Herring A, Ceballos-Diaz C, Das P, Golde TE. Hippocampal expression of murine IL-4 results in exacerbation of amyloid deposition. Mol Neurodegener. 2012; 7:36. [PubMed: 22838967]

95. de la Monte SM. Contributions of brain insulin resistance and deficiency in amyloid-related neurodegeneration in Alzheimer's disease. Drugs. 2012; 72:49–66. [PubMed: 22191795]

96. Cholerton B, Baker LD, Craft S. Insulin resistance and pathological brain ageing. Diabet Med. 2011; 28:1463–1475. [PubMed: 21974744]

97. Bosco D, Fava A, Plastino M, Montalcini T, Pujia A. Possible implications of insulin resistance and glucose metabolism in Alzheimer's disease pathogenesis. J Cell Mol Med. 2011; 15:1807–1821. [PubMed: 21435176]

98. Candeias E, Duarte AI, Carvalho C, Correia SC, Cardoso S, Santos RX, Placido AI, Perry G, Moreira PI. The impairment of insulin signaling in Alzheimer's disease. IUBMB Life. 2012; 64:951–957. [PubMed: 23129399]

99. Craft S, Cholerton B, Baker LD. Insulin and Alzheimer's disease: Untangling the web. J Alzheimers Dis. 2013; 33(Suppl 1):S263–S275. [PubMed: 22936011]

100. Williamson R, McNeilly A, Sutherland C. Insulin resistance in the brain: An old-age or new-age problem? Biochem Pharmacol. 2012; 84:737–745. [PubMed: 22634336]

101. Lee CC, Huang CC, Hsu KS. Insulin promotes dendritic spine and synapse formation by the PI3K/Akt/mTOR and Rac1 signaling pathways. Neuropharmacology. 2011; 61:867–879. [PubMed: 21683721]

102. Martin ED, Sanchez-Perez A, Trejo JL, Martin-Aldana JA, Cano Jaimez M, Pons S, Acosta Umanzor C, Menes L, White MF, Burks DJ. IRS-2 deficiency impairs NMDA receptor-dependent long-term potentiation. Cereb Cortex. 2012; 22:1717–1727. [PubMed: 21955917]

103. Costello DA, Claret M, Al-Qassab H, Plattner F, Irvine EE, Choudhury AI, Giese KP, Withers DJ, Pedarzani P. Brain deletion of insulin receptor substrate 2 disrupts hippocampal synaptic plasticity and metaplasticity. PLoS One. 2012; 7:e31124. [PubMed: 22383997]

104. Porter D, Faivre E, Flatt PR, Holscher C, Gault VA. Actions of incretin metabolites on locomotor activity, cognitive function and *in vivo* hippocampal synaptic plasticity in high fat fed mice. Peptides. 2012; 35:1–8. [PubMed: 22465882]

105. Duarte JM, Agostinho PM, Carvalho RA, Cunha RA. Caffeine consumption prevents diabetes-induced memory impairment and synaptotoxicity in the hippocampus of NONcZNO10/LTJ mice. PLoS One. 2012; 7:e21899. [PubMed: 22514596]

106. Planel E, Tatebayashi Y, Miyasaka T, Liu L, Wang L, Herman M, Yu WH, Luchsinger JA, Wadzinski B, Duff KE, Takashima A. Insulin dysfunction induces *in vivo* tau hyperphosphorylation through distinct mechanisms. J Neurosci. 2007; 27:13635–13648. [PubMed: 18077675]

107. Abbenante G, Kovacs DM, Leung DL, Craik DJ, Tanzi RE, Fairlie DP. Inhibitors of beta-amyloid formation based on the beta-secretase cleavage site. Biochem Biophys Res Commun. 2000; 268:133–135. [PubMed: 10652226]

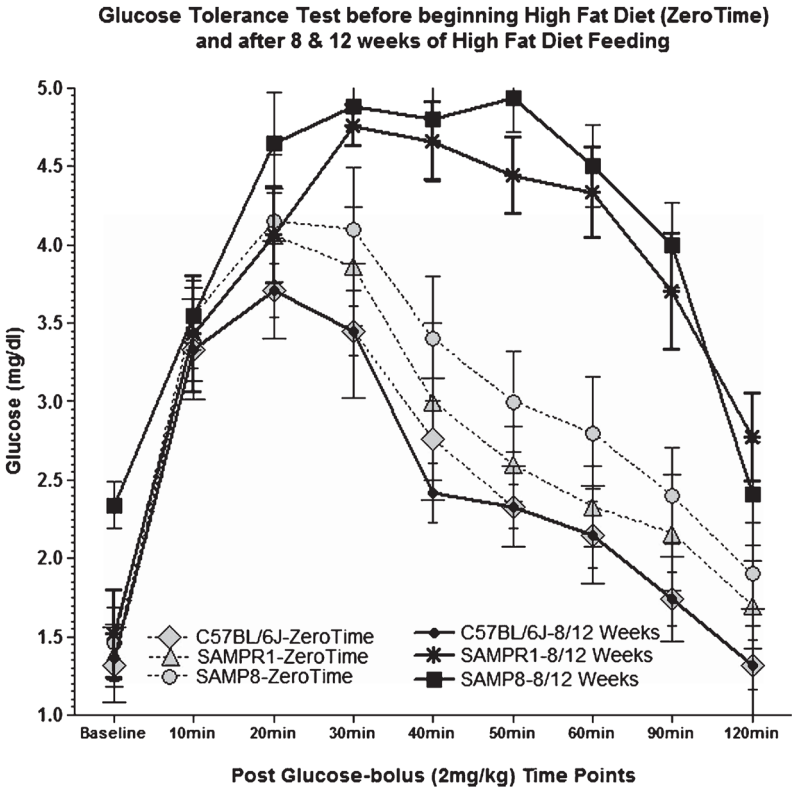

Fig. 1.

Effects of high fat (HF) feeding on glucose tolerance test in SAMP8, SAMPR1, and C57BL/6J mice before beginning HF diet (Zero Time), and after 8/12 weeks of HF feeding, performed after overnight fasting at every 20 min up to 2 h post a single bolus glucose injection (2 mg/kg). Glucose tolerance test at Zero Time shows peaking of blood glucose levels between 20–30 min and quickly normalizing thereafter, suggestive of normal functioning of pancreas. On the other hand, glucose tolerance test after 8/12 weeks of HF diet showed that peaking of blood glucose levels for SAMP8 and SAMPR1 mice, but not for c57BL/6J mice, at 20–30 min, consistently maintained high up to 90 min with a gradual decline by 120 min, indicating failure of pancreas and development of type 2 diabetes, as opposed to normal functioning of pancreas in C57BL/6J mice.

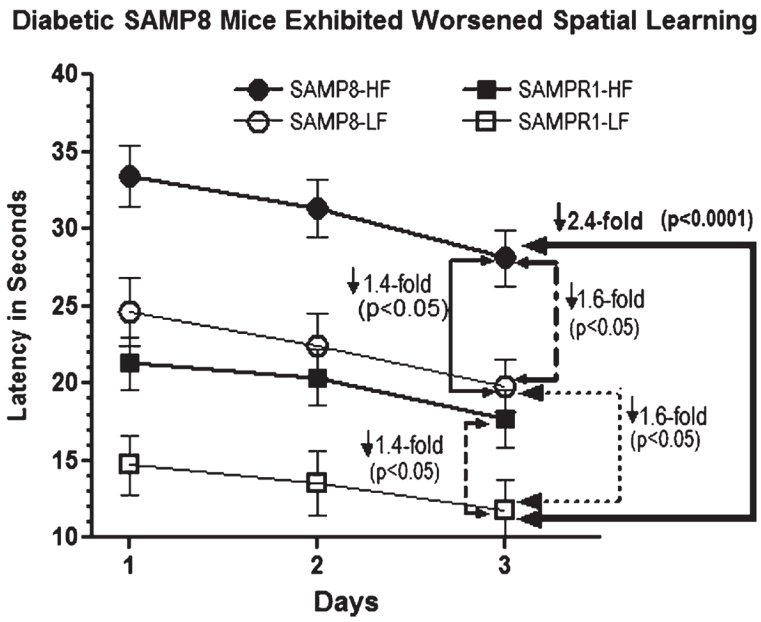

Fig. 2.

Effect of high fat (HF) diet induced experimental T2DM on Morris water maze acquisition learning in SAMP8 and SAMPR1 mice, as measured by latency (Time in seconds required to reach the submerged platform). Data are presented as group means ± standard deviation (SD) derived from the average individual values (6 trials/animal/day for 3 days) for each group. Note that compared to low-fat (LF) fed non-diabetic SAMPR1 mice, spatial acquisition learning was observed to be gradually worsened from HF-fed diabetic SAMPR1 mice (1.4-fold) > LF-fed non-diabetic SAMP8 mice (1.6-fold) > HF-fed diabetic SAMP8 mice (2.4-fold). Data indicate the most significantly deteriorated spatial acquisition learning in diabetic SAMP8 mice.

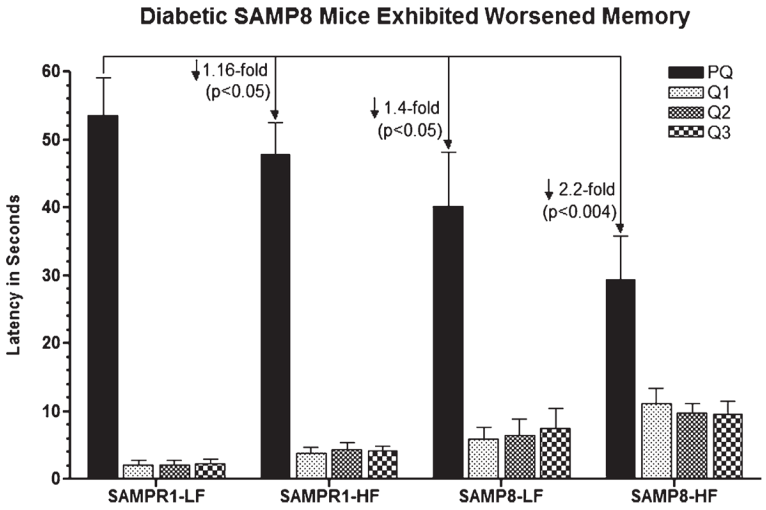

Fig. 3.

Effect of high fat (HF) diet induced experimental T2DM on Morris water maze retention memory in SAMP8 and SAMPR1 mice, as measured by latency (Time in seconds required to explore quadrant of the pool that previously contained platform named PQ). Data are presented as group means ± standard deviation (SD) derived from the average individual values (a single probe trial/animal) for each group. Note that low-fat (LF) fed non-diabetic SAMPR1 mice spent maximum amount of time in PQ, indicating preserved memory of the previously learned location of the platform. By contrast, retention memory was observed to be gradually deteriorated from LF-fed non-diabetic SAMP8 mice > HF-fed diabetic SAMPR1 mice > HF-fed diabetic SAMP8 mice. Data indicate the most significantly deteriorated retention memory in diabetic SAMP8 mice.

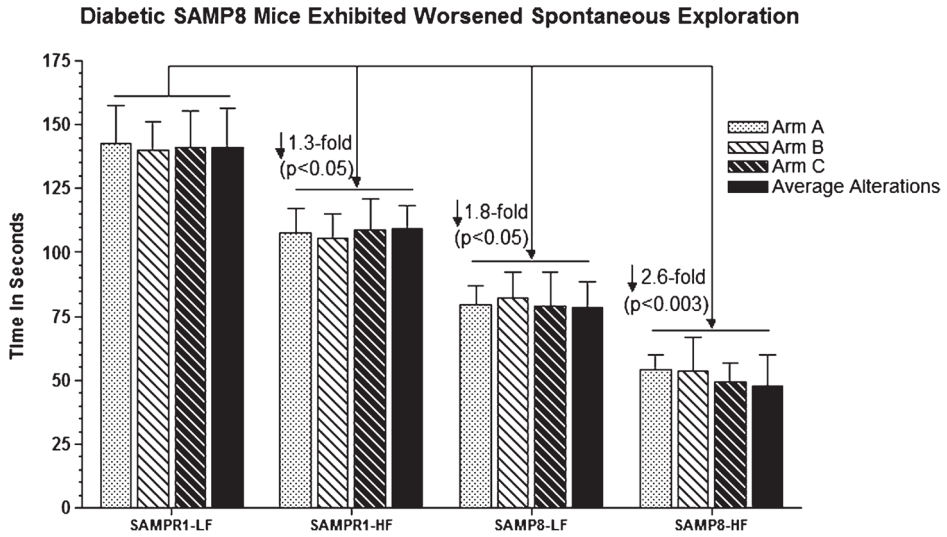

Fig. 4.

Effect of high fat (HF) diet induced experimental T2DM on Y maze spontaneous exploration representing working reference memory in SAMP8 and SAMPR1 mice, as measured by latency (Time in seconds required to explore all arms with average alteration in all arms in Y maze). Data are presented as group means ± standard deviation (SD) derived from the average individual values (a single probe trial/animal) for each group. Note that low-fat (LF) fed non-diabetic SAMPR1 mice spent maximum amount of time in PQ, indicating preserved memory of the previously learned location of the platform. By contrast, retention memory was observed to be gradually deteriorated from HF-fed diabetic SAMPR1 mice > LF-fed non-diabetic SAMP8 mice > HF-fed diabetic SAMP8 mice. Data indicate the most significantly deteriorated retention memory in diabetic SAMP8 mice.

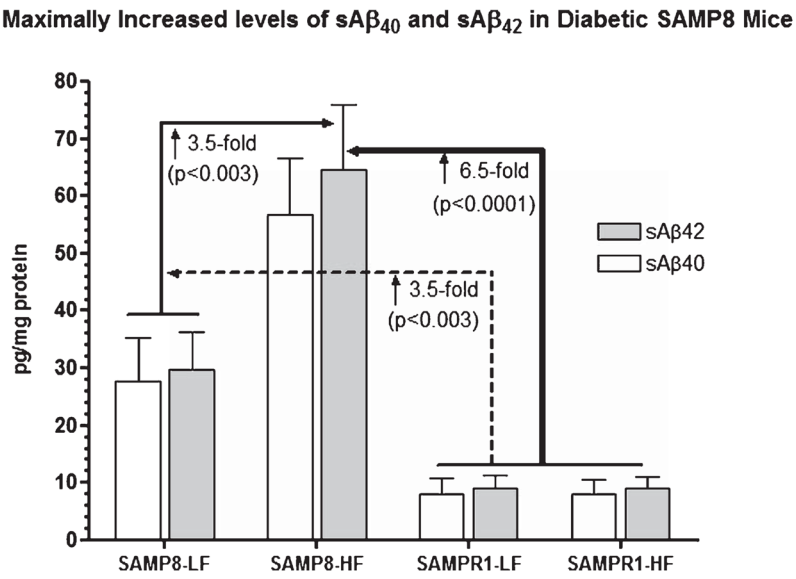

Fig. 5.

Effect of high fat (HF) diet induced experimental T2DM on cerebral levels of Tris-SDS soluble $A\beta_{40}$ ($sA\beta_{40}$) and Tris-SDS soluble $A\beta_{42}$ ($sA\beta_{42}$) in SAMP8 and SAMPR1 mice. Data are presented as group means ± standard deviation (SD) derived from the average individual values for each group. Note that SAMPR1 mice with or without HF diet did not differ significantly exhibiting base levels of cerebral $sA\beta_{40}$ and $sA\beta_{42}$, which were increased by ~3-fold in low-fat (LF) fed non-diabetic SAMP8 mice. HF-fed SAMP8 mice exhibited maximally increased levels of cerebral $sA\beta_{40}$ and $sA\beta_{42}$, both as compared to HF- and LF-fed SAMPR1 mice ($p < 0.0001$), and compared to LF-fed non-diabetic SAMP8 mice ($p < 0.0003$). Data indicate the most significantly increased cerebral $sA\beta_{40}$ and $sA\beta_{42}$ in diabetic SAMP8 mice.

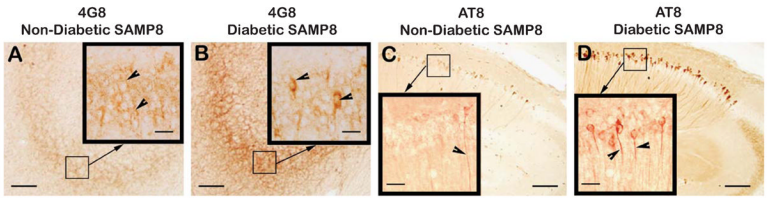

Fig. 6.

Immunodistribution of 4G8 (A, B) and phospho-tau (AT8) (C, D) in the hippocampus of low-fat diet fed non-diabetic SAMP8 mice (A, C), and in the hippocampus of high-fat diet fed diabetic SAMP8 mice (B, D). Note faint 4G8 immunoreactivity within the perikarya of CA3 granule cells (Fig. 6A, inlet, arrowheads) of non-diabetic SAMP8 mice, indicating the presence of intraneuronal Aβ accumulated as a result of accelerated aging in absence of diabetes. Note stronger 4G8 immunoreaction within the perikarya of CA3 granule cells (Fig. 6B, inlet, arrowheads) of diabetic SAMP8 mice, indicating increased accumulation of intraneuronal Aβ than that of non-diabetic SAMP8 mice increased as a result of accelerated aging in presence of diabetes. Similarly, there was observed some evidence of tau phosphorylation within the CA1 hippocampal neurites in non-diabetic SAMP8 mice (Fig. 6C, inlet, arrowhead) merely due to accelerated aging, which was remarkably increased in the CA hippocampal CA1 of diabetic SAMP8 mice (Fig. 6D, inlet, arrowheads) as a result of accelerated aging compounded with diabetes. Scale bars in A-D = 100 μm; Scale bars in all inlets = 20 μm.

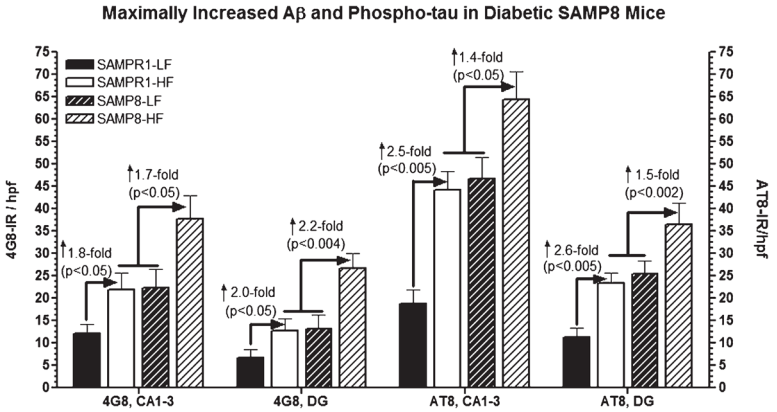

Fig. 7.

Effect of high fat diet induced experimental T2DM on the immunoreactivities (IR) of Aβ (4G8) and phospho-tau (AT8) in the CA1-3 and dentate gyrus (DG) hippocampal subfields of SAMPR1 and SAMP8 mice. Data are represented as group mean ± standard deviation (SD) derived from average individual values for each group. Note that both high fat fed diabetic SAMPR1 mice and low fat fed non-diabetic SAMP8 mice showed more or less similar pattern of 4G8-IR Aβ and AT8-IR phospho-tau within Ca1-3 and DG, which were 1.8–2.0-fold higher for 4G8-IR and 2.5–2.6-fold higher for AT8-IR than the low fat fed non-diabetic SAMPR1 mice. Feeding of high fat diet to SAMP8 mice resulted in 1.7–2.2-fold increase in 4G8-IR Aβ and 1.4–1.5-fold increase in AT8-IR phospho-tau within the respective hippocampal subfields. Data indicate that diabetic SAMP8 mice exhibited Alzheimer-like changes with regard to Aβ and phospho-tau.

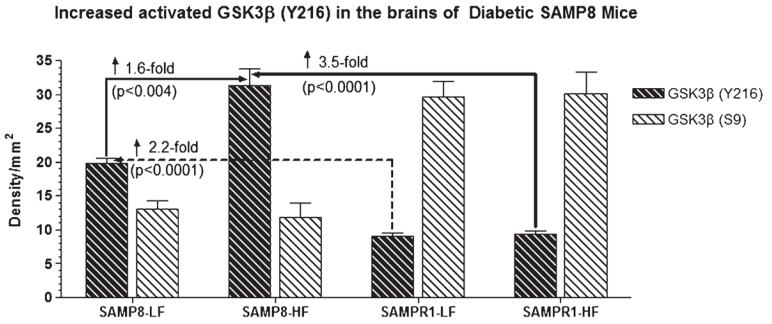

Fig. 8.

Western blot of brain samples derived from SAMP8 or SAMPR1 mice fed with high fat (HF) or low fat (LF) diets showing the reactivity for glycogen synthase kinase-3β (GSK3β) phosphorylated at tyrosine 216 site-activated form of GSK3β (anti-Y216 GSK3β) and at serine 9 site-inactive form of GSK3β (anti-S9 GSK3β) (BioSource International). In general, density for activated GSK3β (Y216) is greater in the brains of SAMP8 mice than that of SAMPR1 mice. By contrast, density for inactive form of GSK3β (S9) is greater in the brains of SAMPR1 mice than that of SAMP8 mice. HF treatment did not affect the reaction for inactive GSK3β (S9) in the brains of SAMP8 mice. HF treatment increased the density for activated GSK3β (Y216) only in the brains of SAMP8 mice, but not in the brains of SAMPR1 mice, indicating that experimental induction of type 2diabetes in SAMP8 mice promotes abnormal phosphorylation of tau. Densitometric analysis showed that compared to LF-fed non-diabetic SAMP8 mice, the levels of GSK3β (Y216) increased by 1.6-fold ($p < 0.004$) in HF-fed diabetic SAMP8 mice. Compared to LF-or HF-fed non-diabetic or diabetic SAMPR1 mice, the levels of GSK3β (Y216) increased by 2.2-fold ($p < 0.0001$) in HF-fed diabetic SAMP8 mice.

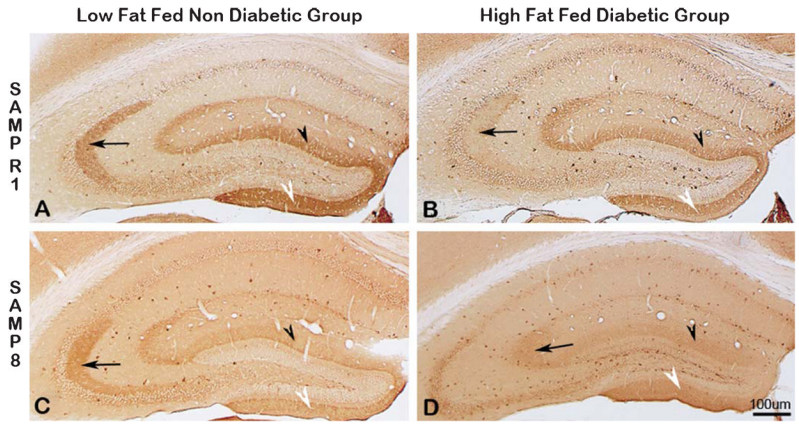

Fig. 9.

Immunodistribution of synaptophysin (SYN) in the hippocampus of SAMPR1 (A, B, top panel), and SAMP8 (C, D, bottom panel); low-fat fed non-diabetic mice (A, C, left panel), and with high-fat fed diabetic mice (B, D, right panel). Note the strongest SYN immunoreactivity (IR) within the CA3 dendritic field (Fig. 9A, arrow), and within the supra-granular (Fig. 9A, black arrowhead) and infragranular (Fig. 9A, white arrowhead) molecular layers of DG of non-diabetic SAMPR1 mice. Note that experimental induction of diabetes in SAMPR1 mice resulted in the reduction of SYN immunoreactivity only in the CA3 dendritic field (Fig. 9B, black arrowhead), while preserving SYN immunoreactivity within the supra-granular (Fig. 9B, black arrowhead) and infragranular (Fig. 9B, white arrowhead) molecular layers of DG of diabetic SAMPR1 mice. On the other hand, in non-diabetic SAMP8 mice, SYN immunoreactivity in the CA3 dendritic field (Fig. 9C, black arrowhead) was preserved, but the SYN immunoreactivity within the supra-granular (Fig. 9C, black arrowhead) and infragranular (Fig. 9C, white arrowhead) molecular layers of DG was reduced. In the hippocampus of diabetic SAMP8 mice, SYN immunoreactivity in all CA3 (Fig. 9D, arrow) and respective DG subfields (Fig. 9D, black arrowhead and white arrowhead) were observed to be greatly reduced. Scale bar = 100 μm.

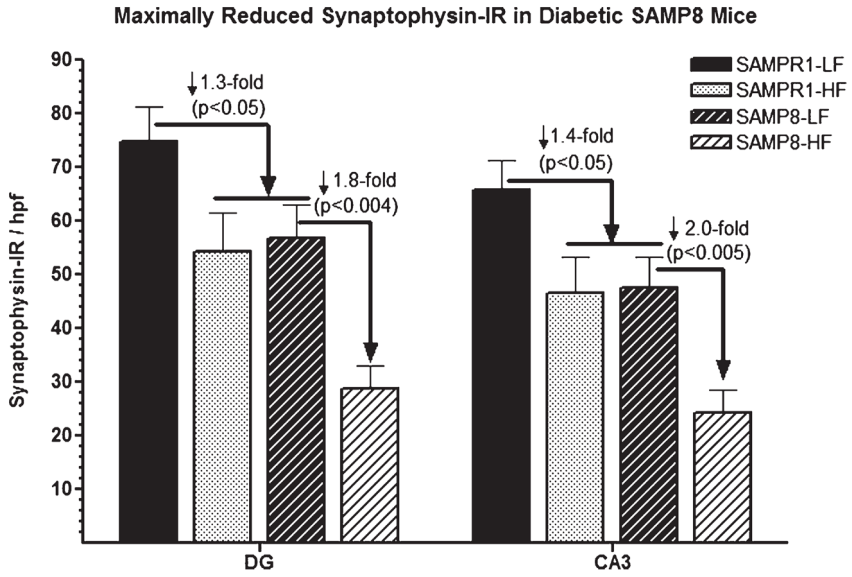

Fig. 10.

Effect of high fat (HF) diet induced experimental T2DM on the immunoreactivities (IR) of synaptophysin (SYN) in the CA3 and dentate gyrus (DG) hippocampal subfields of SAMPR1 and SAMP8 mice. Data are represented as group mean ± standard deviation (SD) derived from average individual values for each group. Note that both HF-fed diabetic SAMPR1 mice and low fat (LF) fed non-diabetic SAMP8 mice exhibited matching pattern of SYN-IR, which were 1.8–2.0-fold lower than the hippocampal SYN-IR observed in the LF-fed non-diabetic SAMPR1 mice. Feeding of HF diet to SAMP8 mice resulted in further reduction of SYN-IR by 1.8–2.0-fold in respective hippocampal of diabetic SAMP8 mice. Data indicate that diabetic SAMP8 mice showed Alzheimer-like synaptic deficits.

J Alzheimers Dis. Author manuscript; available in PMC 2014 March 04.

Table 1

Effect of high-fat (HF) or low-fat (LF) diet on the levels of serum insulin (μg/l), blood HbA1c (%), brain insulin (pg/mg), cytochrome c oxidase, and pyruvate dehydrogenase (pg/mg) in SAMP8 and SAMPR1 mice

Groups	Baseline Prior dietary treatment	1 wk post to dietary treatment	2 wks post dietary treatment	3 wks post dietary treatment	4 wks post dietary treatment	5 wks post dietary treatment	6 wks post dietary treatment	7 wks post dietary treatment	8 wks post dietary treatment	12 wks post dietary treatment
Non-diabetic SAMP8 fed with LF	1.3 ± 0.1[*] 1.9%[#]	1.5 ± 0.2 1.8%[#]	1.7 ± 0.5 2.0%[#]	1.9 ± 0.5 1.9%[#]	2.1 ± 0.2 2.1%[#]	2.3 ± 0.1 2.0%	2.7 ± 0.3 2.1%	2.9 ± 0.4 2.0%	3.1 ± 0.1 2.1%	2.9 ± 0.2 2.1% 0.8 ± 0.04[@] 1.9 ± 0.03[**] 1.8 ± 0.01[^]
Diabetic SAMP8 fed with HF	1.4 ± 0.4 1.8%[#]	1.8 ± 0.2 2.1%[#]	2.1 ± 0.1 2.1%[#]	2.6 ± 0.2 2.4%[#]	2.9 ± 0.2 3.2%[#]	3.7 ± 0.3 3.8%[#]	4.1 ± 0.1 4.2%[#]	4.4 ± 0.6 5.6%[#]	5.1 ± 0.1 5.9%[#]	4.9 ± 0.1 6.2%[#] 1.9 ± 0.02[@] 1.1 ± 0.06[**] 0.8 ± 0.04[^]
Non-diabetic SAMPR1 fed with LF	1.3 ± 0.2 1.8%[#]	1.6 ± 0.4 1.9%[#]	1.8 ± 0.3 1.8%[#]	1.9 ± 0.2 2.0%[#]	2.3 ± 0.4 1.9%[#]	2.4 ± 0.2 2.0%[#]	2.8 ± 0.3 2.0%[#]	2.9 ± 0.2 1.9%[#]	3.0 ± 0.2 2.0%[#]	2.8 ± 0.2 2.0%[#] 0.9 ± 0.02[@] 1.8 ± 0.06[**] 1.8 ± 0.04[^]
Diabetic SAMPR1 fed with HF	1.4 ± 0.1 1.8%[#]	1.7 ± 0.2 1.9%[#]	2.2 ± 0.3 2.1%[#]	2.8 ± 0.2 2.1%[#]	3.1 ± 0.1 2.6%[#]	3.6 ± 0.2 3.7%[#]	4.0 ± 0.2 4.1%[#]	4.5 ± 0.2 5.4%[#]	5.0 ± 0.3 6.1%[#]	4.6 ± 0.3 6.1%[#] 1.8 ± 0.04[@] 1.2 ± 0.06[**] 0.9 ± 0.04[^]

[*] Serum insulin;

[#] % Blood HbA1c;

[@] Brain insulin;

[**] Cytochrome c oxidase;

[^] Pyruvate dehydrogenase.